APPLIED ORGANOMETALLIC CHEMISTRY
Appl. Organometal. Chem. 2007; **21**: 909–912
Published online 7 August 2007 in Wiley InterScience
(www.interscience.wiley.com) DOI:10.1002/aoc.1300

Preparation of size-controlled In_2O_3 nanoparticles†

Peng Zhu, Weiya Wu, Jianping Zhou and Wu Zhang*

College of Chemistry and Materials Science, Anhui Normal University, Wuhu, Anhui 241000, People's Republic of China

Received 26 April 2007; Revised 26 May 2007; Accepted 3 June 2007

Highly crystalline and monodisperse In_2O_3 nanoparticles were successfully prepared by thermal decomposition of $In(dipy)_3Cl_3{\cdot}2H_2O$ in oleylamine and oleic acid under inert atmosphere. The size of In_2O_3 nanoparticles could be readily tuned from 10–15 nm to 40–50 nm, depending on the molar ratio of precursor to combined solvent in the reaction system. As-synthesized In_2O_3 nanoparticles have a center-body cubic structure as characterized by powder X-ray diffraction and selected-area electron diffraction. Transmission electron microscopy images showed that In_2O_3 nanoparticles have a narrow size distribution. A relatively strongly PL peak centered at 378 nm could be clearly seen when 10–15 nm In_2O_3 nanoparticles redispersed in cyclohexane were excited at 275 nm at room temperature. Copyright © 2007 John Wiley & Sons, Ltd.

KEYWORDS: indium oxide; nanoparticles; size-controlled; luminescence

INTRODUCTION

Metal oxide nanocrystals have a wide range of applications in magnetic data storage, battery materials, catalysts and sensors.[1] In particular, indium oxide nanocrystals are potentially important in microelectronic device materials in solar cells,[2] flat-panel displays, sensors,[3,4] transparent conductors[5] and architectural glasses.

The thermolysis of molecular precursors in hot surfactant solutions is one of the most effective methods for preparing highly crystalline and size-controlled metal oxide nanocrystals. A lot of metal oxide nanocrystals have been prepared by the thermal decomposition of metal acetylacetonates in oleylamine.[6–9] Other available molecular precursors developed for metal or metal oxide nanoparticles include metal acetates,[10,11] metal formates,[12] metal oleates[13] and organometallic precursors.[14,15] Few molecular precursors have been reported for In_2O_3 nanocrystals synthesis by thermal decomposition in oleylamine.[6,10,16] Therefore developing new, simple, cheap, air-stable and low-toxicity precursors to nano-indium oxide with good size control is of considerable interest. Herein we report the synthesis of quasi-monodisperse size-controlled In_2O_3 nanocrystals (NCs) from thermal decomposition of $In(dipy)_3Cl_3{\cdot}2H_2O$ (dipy = α, α-dipyridyl) precursor in the presence of stabilizing surfactants oleylamine and oleic acid.

*Correspondence to: Wu Zhang, College of Chemistry and Materials Science, Anhui Normal University, Wuhu, Anhui 241000, People's Republic of China.
E-mail: zhangwu@mail.ahnu.edu.cn
Contract/grant sponsor: Educational Office of Anhui Province; Contract/grant number: 2006kj147B.
Contract/grant sponsor: Anhui Normal University.
†This article was published online on 7th August 2007. An error was subsequently identified and corrected by an erratum notice that was published online on DOI 1332. This printed version incorporates the amendment identified by the erratum notice.

EXPERIMENTAL

Materials

All reagents are analytically pure. $InCl_3{\cdot}4H_2O$, α,α-dipyridyl, dichloromethane, ethanol and cyclohexane were purchased from Shanghai Chemical Company. oleylamine (70%) and oleic acid (90%) were obtained from Alfa.

Preparation of precursor $In(dipy)_3Cl_3{\cdot}2H_2O$

A 0.3 g (1.02 mmol) aliquot of $InCl_3{\cdot}4H_2O$ was dissolved in 10 ml distilled water in a 50 ml beaker. Then 15 ml ethanol solution containing 0.5 g (3.20 mmol) α,α-dipyridyl was added drop-wise with constant stirring for 2 h. The white precipitate formed was centrifuged, rinsed with ethanol, then rinsed with distilled water repeatedly. Finally it was dried at 60 °C for 4 h.

Preparation of 10–15 nm In_2O_3 nanoparticles

A 0.18 g (0.25 mmol) aliquot of $In(dipy)_3Cl_3{\cdot}2H_2O$, with 5.5 ml (12 mmol) oleylamine (70%) and 4 ml (12.3 mmol) oleic acid (90%), was added to a three-necked flask equipped with a condenser at room temperature. Ar was bubbled through the solution for 20 min and then the solvents were repeatedly evacuated to remove oxygen and water at about 100 °C for

5 min. Then the flask was then heated to 290 °C at a heating rate of 15 °C min^{-1} for 7 h under an Ar atmosphere. When the temperature of this reaction system was increased to 100 °C, the color was light yellow. When the temperature was further increased to 240 °C, the mixture gradually changed to a brown turbid slurry. Finally, when the temperature was 290 °C, the color became dark brown. After cooling the resulting solution to room temperature, a dark-brown viscous oil formed. Dichloromethane (10 ml) was added to enhance the fluidity of the reaction mixture. To the resulting brown solution was added excess ethanol (40 ml) to form a pale yellow precipitate. After centrifugation and repeated washing with ethanol, a pale yellow powder of 10–15 nm In_2O_3 nanocrystals [Fig. 2(b)] was obtained, which could be easily redispersed in various organic solvents such as cyclohexane and toluene.

Preparation of 40–50 nm In_2O_3 nanoparticles

A similar procedure was used to obtain 40–50 nm In_2O_3 nanoparticles [Fig. 2(a)]: 0.18 g (0.25 mmol) $In(dipy)_3Cl_3{\cdot}2H_2O$, 2.9 ml (6 mmol) oleylamine (70%) and 2 ml (6 mmol) oleic acid (90%).

Characterization of In_2O_3 nanocrystals

The synthesized products were characterized by X-ray powder diffraction (Shimadzu XRD-6000) with graphite monochromatized Cu-Kα radiation ($\lambda = 0.15406$ nm), employing a scanning rate of 0.02° s^{-1} in the 2θ range from 10 to 80°. Figure 1 presents XRD patterns of two samples, a and b, indicating a cubic phase from these NCs because all of the detectable diffraction peaks can be indexed to center-body cubic In_2O_3 (ICDD PDF card no. 71–2195). Figure 1(c) presents the XRD patterns of 40–50 nm In_2O_3 nanoparticles annealed at 400 °C for 2 h.

Transmission electron microscopy (TEM) images and selected-area electronic diffraction (SAED) patterns were taken on a Hitachi Model H-800 instrument with a tungsten filament, using an accelerating voltage of 200 kV. The specimen of TEM and high-resolution TEM (HRTEM) measurements were prepared by spreading a droplet of cyclohexane suspension of In_2O_3 nanoparticles onto a copper grid and allowing it to dry in air. Nearly monodisperse spherical nanoparticles around 40–50 nm in diameter were shown in Fig. 2(a). Smaller nanoparticles 10–15 nm in diameter were shown in Fig. 2(b). Figure 2(c) presented the TEM micrograph of 40–50 nm In_2O_3 nanoparticles annealed at 400 °C for 2 h. The size of the nanoparticles was calculated from TEM images.

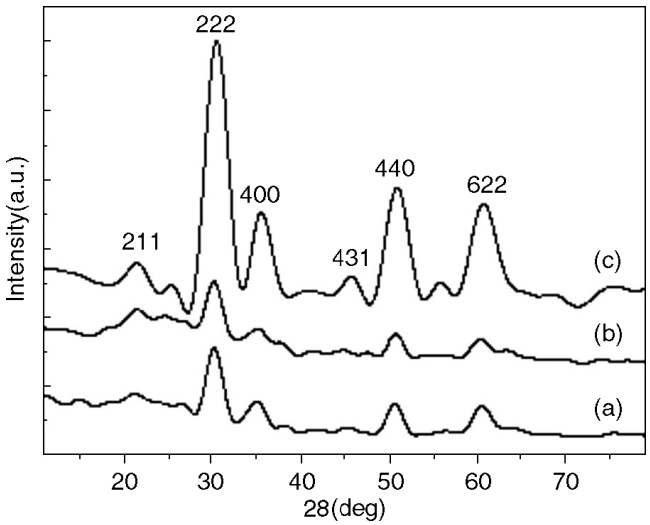

Figure 1. X-ray diffraction of (a) 40–50 nm, (b) 10–15 nm center-body In_2O_3 nanoparticles (ICDD PDF card NO.71–2195) and (c) 40–50 nm center-body In_2O_3 nanoparticles annealed at 400 °C for 2 h.

The HRTEM images were taken on a Jeol-2010 high-resolution TEM performed at 200 kV. An interplanar distance of 0.296 nm close to the {222} lattice spacing of the cubic phase In_2O_3 was obtained.

The photoluminescence spectrum was recorded on a Hitachi F-4500 fluorescence spectrometer. To explore the PL emissions property, 10–15 nm In_2O_3 nanoparticles dispersed in cyclohexane were excited at 275 nm at room temperature. Figure 4 shows a relatively strong PL peak centered at 378 nm.

RESULTS AND DISCUSSION

TEM image of the powder obtained using a 1 : 24 molar ratio of precursor/combined solvent is shown in Fig. 2(a). Nearly

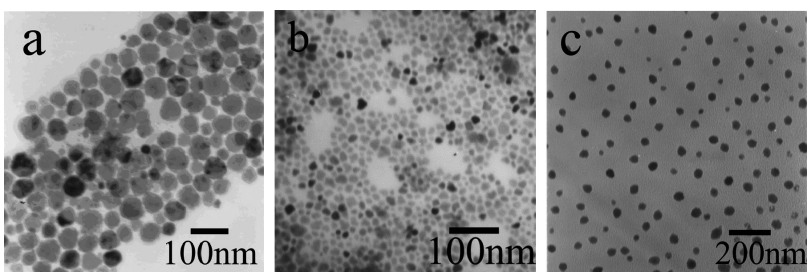

Figure 2. TEM micrograph of (a) 40–50 nm, (b) 10–15 nm In_2O_3 nanoparticles and (c) 40–50 nm In_2O_3 nanoparticles annealed at 400 °C for 2 h.

DOI: 10.1002/aoc

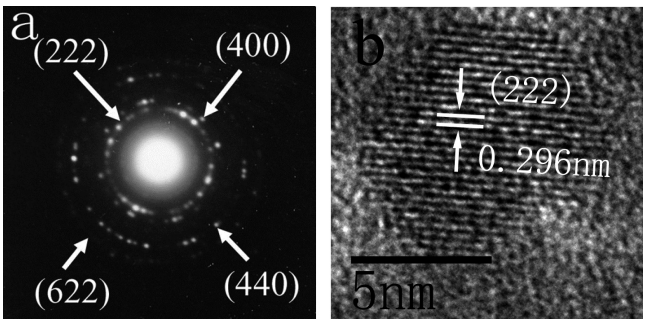

Figure 3. SAED pattern (a) and HRTEM (b) image of the 10 nm In_2O_3 nanoparticles.

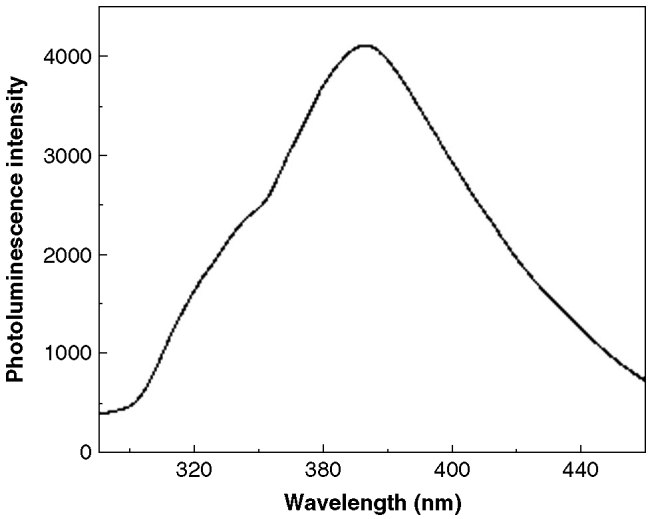

Figure 4. Photoluminescence spectra of 10–15 nm In_2O_3 nanoparticles.

monodisperse spherical nanoparticles around 40–50 nm in diameter were observed. The size of In_2O_3 nanoparticles can easily be tuned by changing the ratio of precursor to combined solvent. Smaller nanoparticles around 10–15 nm in diameter were obtained as shown in Fig. 2(b) when a 1 : 48 molar ratio of precursor/combined solvent was used. The SAED pattern of the 10–15 nm nanoparticles shown in Fig. 3(a) is consistent with the (222), (400), (440) and (622) planes of body-cubic In_2O_3. This is also consistent with the XRD data given in Fig. 1. The HRTEM image shown in Fig. 3(b) reveals an interplanar distance of 0.296 nm close to the {222} lattice spacing of the cubic phase In_2O_3. HRTEM proved our product highly crystalline nanoparticles.

In this experiment, combined solvent in a molar ratio of oleylamine to oleic acid of 1 : 1 was adopted owing to the fact that the presence of an appropriate amount of oleic acid could further narrow the polydispersity of the product compared with the use of oleylamine alone.[10]

To investigate how the synthetic conditions influence product nanoparticles, it is be helpful if the particle size distribution can be found to vary closely with changes in variables adopted in the reaction. For particles prepared by our present approach, it is simple to find such effects from TEM images, from changes in the molar ratio adopted in the reaction.

The mechanism of shape-controlled synthesis of nanocrystals is being investigated intensively.[17–20] During the thermolysis of the precursor complexes, the capping ligands have distinct effects on the shape of the products formed during the crystal-growth process.[19–22] The thermolysis of precursor complexes releases a large number of indium oxide nuclei. The oxygen coming from crystal water of the precursor acts as the oxidant during the nucleation course of In_2O_3 nanoparticles. The amount of surfactants adsorbing on the surface of nuclei will determine the size of the products. When more surfactants are added, the indium oxide nuclei face with a higher density of surface atoms is blocked by the adsorption of plentiful surfactants during the growth of colloidal nanocrystals, and the growth along the surface is therefore considerably restricted. Therefore smaller nanoparticles are obtained when more surfactants are used.

To investigate how the solvent influences the product, we designed another two experiments. We found that using oleic acid without oleylamine did not result in any NCs, whereas a high content of oleylamine without oleic acid led to rapid growth and aggregation of NCs, which can be seen from the TEM image. In our case, experiments show that oleic acid binds more strongly then oleylamine to the surface atoms of the nanocrystals due to its higher oxophilicity. Therefore, the combined solvent is a key factor in forming In_2O_3 NCs in this experiment.

It is well known that the bulk In_2O_3 cannot emit light at room temperature.[23] However, PL emissions of the nanostructured In_2O_3 due to the effect of the oxygen vacancies have been widely reported.[24,25]The oxygen-deficiency can act as donors and would induce the formation of new energy levels in the band gap, which results in photoluminescence (PL) under the photoexcitation process.[10] Although the PL emission mechanism of In_2O_3 is still ambiguous, it is believed that the blue PL peaks found in previous works are mainly attributed to deeper energy level emission at room temperature. In Fig. 4, a relatively strong PL peak centered at 378 nm can be clearly seen when 15 nm In_2O_3 nanoparticles dispersed in cyclohexane are excited at 275 nm at room temperature. The In_2O_3 nanoparticle samples described in this paper do not show PL emission at lower energies ($\sim$ 400–520 nm) due to amorphous In_2O_3 or oxygen vacancies, as observed for other previously reported In_2O_3 nanoparticles[24] and nanowires.[26, 27]

CONCLUSIONS

In conclusion, we have prepared In_2O_3 nanocrystals by thermal decomposition of a single precursor $In(dipy)_3Cl_3{\cdot}2H_2O$ in oleylamine and oleic acid under inert atmosphere. The sizes

DOI: 10.1002/aoc

of the In_2O_3 nanoparticles were well controlled by changing the ratio of precursor to combined solvent. PL spectra showed that the as-obtained In_2O_3 are highly crystalline and defect-free, which is beneficial for its application in optic and electronic devices.

Acknowledgments

The financial support received from the Educational Office of Anhui Province, 2006kj147B, and Anhui Normal University is appreciated.

REFERENCES

1. Zeng H, Liu JP, Wang ZL, Sun S. *Nature* 2002; **420**: 395. DOI: 10.1038/nature01208.
2. Gopchandran KG, Joseph B, Abraham JT, Koshy P, Vaidyan VK. *Vacuum* 1997; **48**: 547. DOI: 10.1016/S0042-207X(97)00023-7.
3. Zhang D, Li C, Liu X. Han S, Tang T, Zhou C. *Appl. Phys. Lett.* 2003; **83**: 1845. DOI: 10.1063/1.1604194.
4. Zhang D, Liu Z, Li C, Tang T, Liu X, Han S, Lei B, Zhou C. *Nano Lett.* 2004; **4**: 1919. DOI: 10.1021/nl0489283.
5. Wan Q, Dattoli EN, Fung WY, Guo W, Chen Y, Pan X, Lu W. *Nano Lett.* 2006; **6**: 2909. DOI: 10.1021/nl062213d.
6. Park JT, Seo WS, Jo HH, Lee K. *Adv. Mater.* 2003; **15**: 795. DOI: 10.1002/adma.200304568.
7. Park JT, Seo WS, Shim JH, Oh SJ, Lee EK, Hur NH. *J. Am. Chem. Soc.* 2005; **127**: 6188. DOI: 10.1021/ja050359t.
8. Sun SH, Zeng H. *J. Am. Chem. Soc.* 2002; **124**: 8204. DOI: 10.1021/ja026501x.
9. Won SS, Hyong HJ, Kwangyeol L, Bongsoo K, Sang JO, Joon TP. *Angew. Chem.* 2004; **116**: 1135. DOI: 10.1002/ange.200352400.
10. Liu QS, Lu WG, Ma AH, Tang JK, Lin J, Fang JY. *J. Am. Chem. Soc.* 2005; **127**: 5276. DOI: 10.1021/ja042550t.
11. Ming Y, Yi G, Igor LK, Tamar A, Zhu YM, Neumark GF, Stephen OB. *J. Am. Chem. Soc.* 2004; **126**: 6206. DOI: 10.1021/ja031696+.
12. Sun X, Zhang YW, Si R, Yan CH. *Small* 2005; **1**: 1081. DOI: 10.1002/small.200500119.
13. An KJ, Lee N, Park J, Sung CK, Hwang Y, Park JG, Kim JY, Park JH, Han MJ, Yu J, Hyeon T. *J. Am. Chem. Soc.* 2006; **128**: 9753. DOI: 10.1021/ja0608702.
14. Bunge SD, Boyle TJ, Headley TJ. *Nano Lett.* 2003; **3**: 901. DOI: 10.1021/nl034200v.
15. Puntes VF, Zanchet D, Erdonmez CK, Alivisatos AP. *J. Am. Chem. Soc.* 2002; **124**: 12874. DOI: 10.1021/ja027262g.
16. Lee CH, Kim M, Kim T, Kim A, Paek J, Lee JW, Lee K. *J. Am. Chem. Soc.* 2006; **128**: 9326. DOI: 10.1021/ja063227o.
17. Cheon J, Kang NJ, Lee SM, Lee JH, Yoon JH, Oh SJ. *J. Am. Chem. Soc.* 2004; **126**: 1950. DOI: 10.1021/ja038722o.
18. Zeng H, Rice PM, Wang SX, Sun S. *J. Am. Chem. Soc.* 2004; **126**: 11458. DOI: 10.1021/ja045911d.
19. Si R, Zhang YW, You LP, Yan CH. *Angew. Chem.* 2005; **117**: 3320. DOI: 10.1002/ange.200462573.
20. Pinna N, Garnweitner G, Antonietti M, Niederberger M. *J. Am. Chem. Soc.* 2005; **127**: 5608. DOI: 10.1021/ja042323r.
21. Yang SW, Gao L. *J. Am. Chem. Soc.* 2006; **128**: 9330. DOI: 10.1021/ja063227o.
22. Zhao NN, Pan DC, Nie W, Ji XL. *J. Am. Chem. Soc.* 2006; **128**: 10118. DOI: 10.1021/ja0612145.
23. Ohhata Y, Shinoki F, Yoshida S. *Thin Solid Films* 1979; **59**: 255. DOI: 10.1016/0040-6090(79)90298-0.
24. Zhou HJ, Cai WP, Zhang LD. *Appl. Phys. Lett.* 1999; **75**: 495. DOI: 10.1063/1.124427.
25. Zhang J, Qing X, Jiang F, Dai Z. *Chem. Phys. Lett.* 2003; **371**: 311. DOI: 10.1016/S0009-2614(03)00272-0.
26. Liang CH, Meng GW, Lei Y, Phillipp F, Zhang LD. *Adv. Mater.* 2001; **13**: 1330. DOI: 10.1002/1521-4095.
27. Zheng MJ, Zhang LD, Li GH, Zhang XY, Wang XF. *Appl. Phys. Lett.* 2001; **79**: 839. DOI: 10.1063/1.1389071.